

Estimation of the stiffness tensor in organic-rich mudrock Vaca Muerta by integrating core data with Rock Physics models

Juan E. Santos

Universidad de Buenos Aires (UBA) Argentina and Purdue University, Indiana, USA

In collaboration with A. Sánchez Camus (Solaer Ingeniería, UNLP, Argentina), G. B. Savioli (UBA, Argentina) and P. M. Gauzellino (UNLP, Argentina)

**SEG Rock Physics and Geofluid Detection Workshop,
December 2025,
Hohai University, Nanjing, China**

Characterization of ultra-low permeability organic-rich mudrock reservoirs. I

- This work presents a methodology to characterize and analyze the lower section of the Vaca Muerta Formation (VMF) in the Neuquén Basin, Argentina.
- A core sample, 18 meters in length, was extracted between 3092 and 3110 m TVD. Sections were cut at 0, 45 and 90 degrees relative to bedding, with orientation aligned to the S-wave polarization direction to enable traveltimes measurements of P, SH and SV wave propagation modes. Transducers were affixed to the top and bottom of each sample to ensure accurate acquisition (Geophysics, 57(5), 1992).
- Ultrasonic phase velocity measurements, at frequencies 1 MHz for P-waves and 0.5 MHz for S waves, exhibited a clear **vertical transverse anisotropy (VTI)** behavior in the formation.

Well in the VMF from where the core was extracted

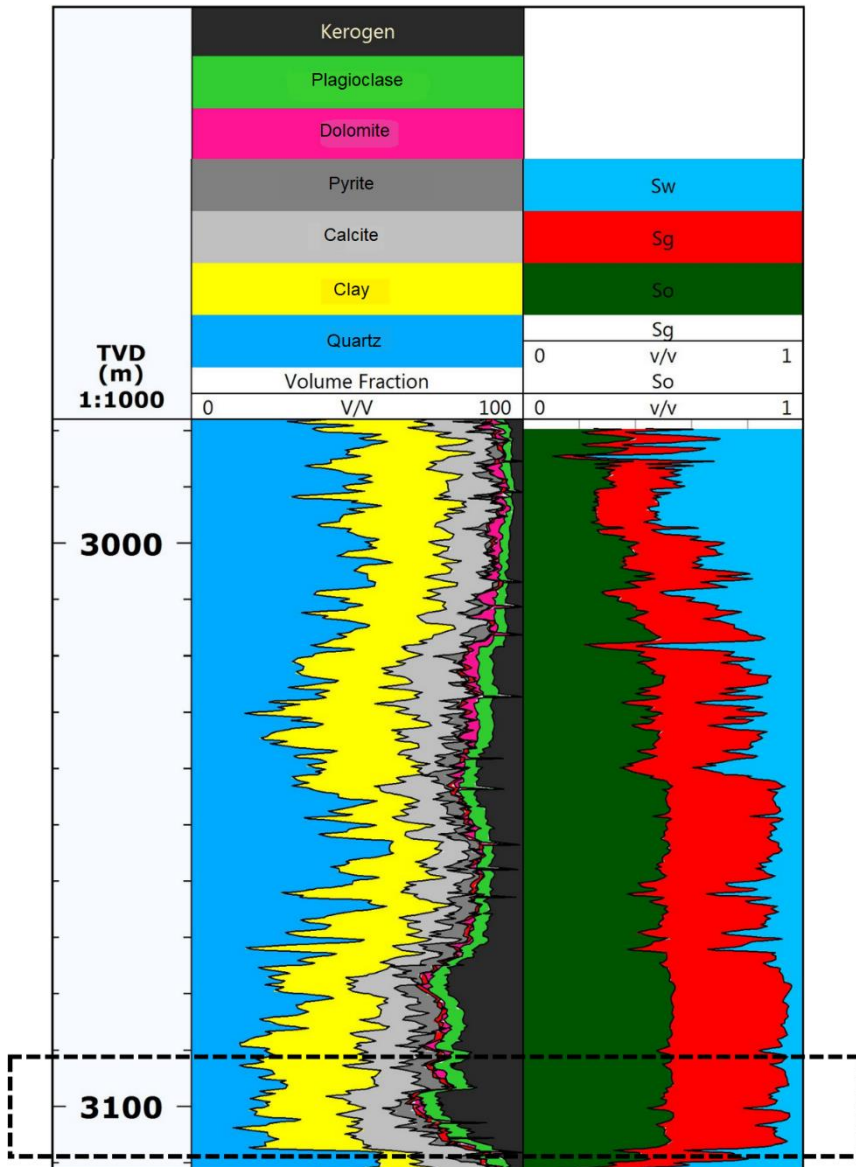
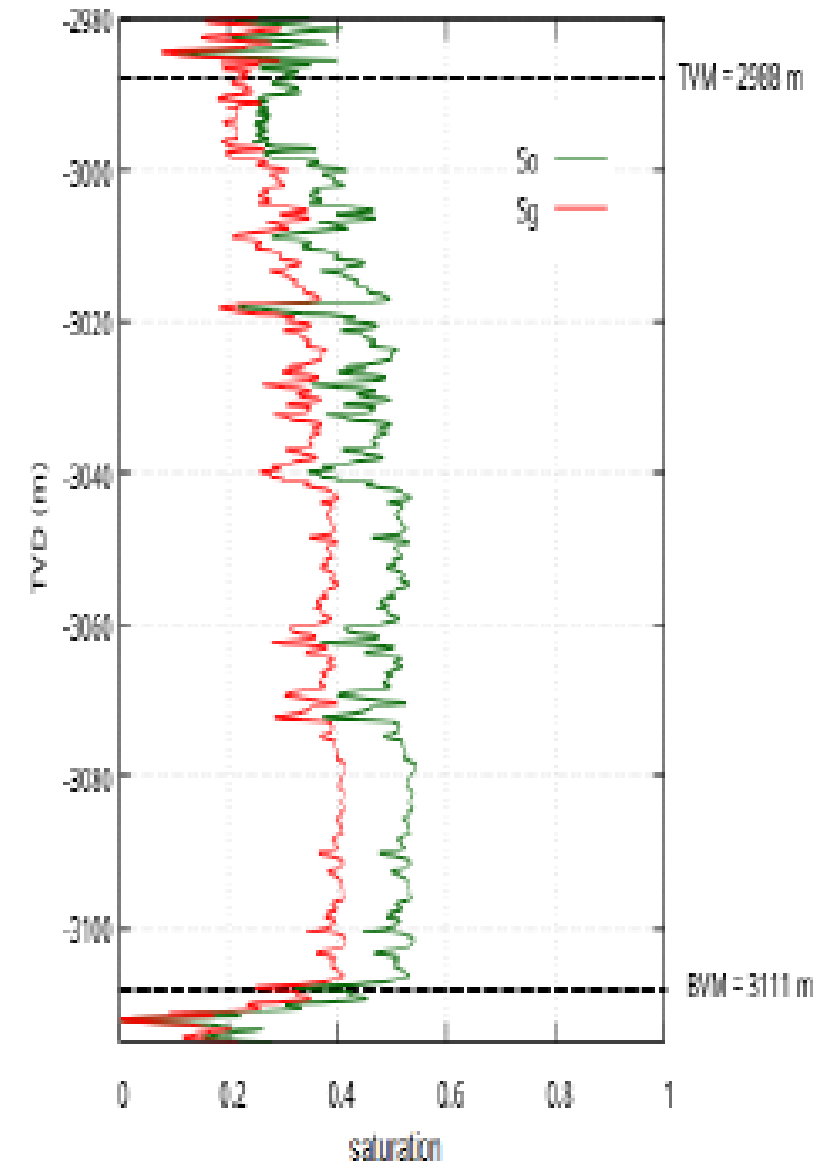


Fig. 1 - VMF mineral composition, kerogen proportions and fluid saturations as function of depth in the well under study. The cored interval is indicated by dotted lines. VMF exhibits a stratified microstructure, in which clay platelets and kerogen are **aligned parallel or sub-parallel to bedding.**

Cored Interval



Characterization of ultra-low permeability organic-rich mudrock reservoirs. II

- VMF is modeled as a periodic sequence of very thin horizontal porous materials, **Material 1** and **2**, where **Biot's theory in the diffusive frequency range** is applicable.
- For both materials porosity is 6 percent and permeability is $2.75 \cdot 10^{-18} \text{ m}^2$.
- **Material 1** is a complex, multimineral assemblage composed of seven solid phases, including 23 percent of kerogen, which is treated as a solid mineral constituent.
- **Material 2** is composed entirely of pure kerogen.

Characterization of ultra-low permeability organic-rich mudrock reservoirs. III

- For horizontally homogeneous material and fluid flow normal to the bedding, the complex VTI stiffness coefficients of the equivalent VTI medium were determined using an analytic solution (CMAME, 283, 2015).
- For patchy saturation, the Finite Element method was used to compute phase velocities and attenuation of '33' waves for a range of frequencies of interest. The compressional p33-experiment (compression normal to bedding) was applied to the representative sample used in the dry case, but now saturated with patchy gas-oil fluid distribution.

Characterization of ultra-low permeability organic-rich mudrock reservoirs. IV

- For **Material 1** a frame bulk modulus of 29.19 GPa and a shear modulus of 17.78 GPa were obtained using a generalized Krief's model. This procedure takes into account the bulk and shear moduli of the individual minerals and their volume fractions (Geophysics, 70 (2), 2005). These moduli values lie within the Hashin–Shtrikman bounds.
- **Material 2** is composed entirely of pure kerogen with grain modulus 7 GPa, density 1400 kg/m³, frame bulk modulus 1.29 GPa and shear modulus 0.36 GPa.

Table 1. Fluid properties

fluid	Bulk modulus (Pa)	Density (kg/m ³)	Viscosity (Pa . s)
Air	1.01325e5	1.225	1.805e-5
Water	2.25e9	1000	0.001
Oil	0.57e9	700	0.01
Gas	0.022e9	78	0.000015

Table 2. Mineralogical properties obtained from X-ray diffraction (XRD) analysis of core sample, used for Material 1 at an effective pressure of 17.23 MPa

mineral	Bulk modulus (GPa)	shear modulus (GPa)	Density (kg/m ³)	Proportions
kerogen	7.0	2.	1400	0.23
Clay	25	9	2700	0.3727
Quartz	45	55	2700	0.1461
Calcite	80	40	2800	0.1068
Plagioclase	80	40	2800	0.0257
Dolomite	100	50	2900	0.0237
Pyrite	170	110	5000	0.035

Computed velocities using dry-core data

The analytic computations were performed on a dry, square sample with a side length of 0.6 mm, consisting of a **periodic sequence composed of 69 layers of Material 1 and one layer of Material 2 per period**.

Table 3 summarizes the results of the VTI analysis, showing a very good agreement between the simulated and laboratory-measured phase velocities, with relative errors remaining below 8 percent.

Table 3. Phase velocities computed, measured and error percentage

Phase velocity v_p (m/s)	Computed	Measured	Percentage error
v_{11} (1 MHz)	4670.87	4331.00	7.80 %
v_{33} (1 MHz)	4015.49	4217.47	4.79 %
v_{55} (0.5 MHz)	2127.41	2193.61	3.01 %
v_{66} (0.5 MHz)	2747.31	2581.00	6.40 %

Table 4. Complex stiffness coefficients p_{ij} (GPa).

p_{11} (1 MHz) = (50.68, 0.000027)
p_{13} (1 MHz) = (12.42, 0.000008)
p_{33} (1 MHz) = (37.46, 0.000235)
p_{55} (0.5 MHz) = (10.51, 0.0)
p_{66} (0.5 MHz) = (17.53, 0.0)

Figures 2 and 3 present polar plots of the phase and energy velocities for the qP, qSV, and SH waves in the dry sample.

Polar representation of qP, qSV and SH phase velocities. Dry core sample

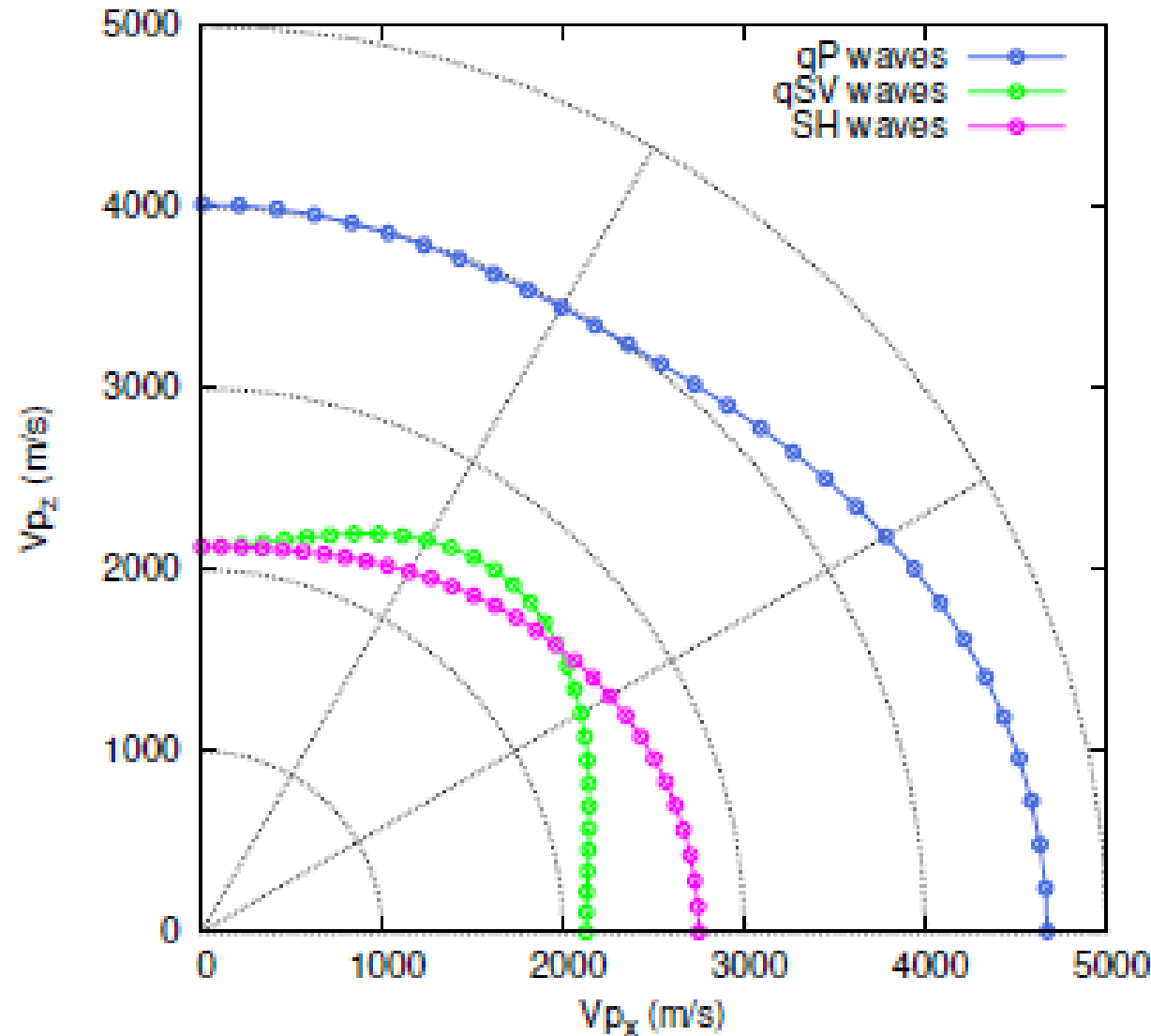


Fig. 2: Polar representation of phase velocities of qP, qSV and SH waves. 0 and 90 degrees indicate waves traveling parallel and normal to the bedding, respectively. Strong VTI behavior is observed. Frequency is 1 MHz for P-waves and 500 kHz for S-waves.

Polar representation of qP, qSV and SH energy velocities. Dry core sample.

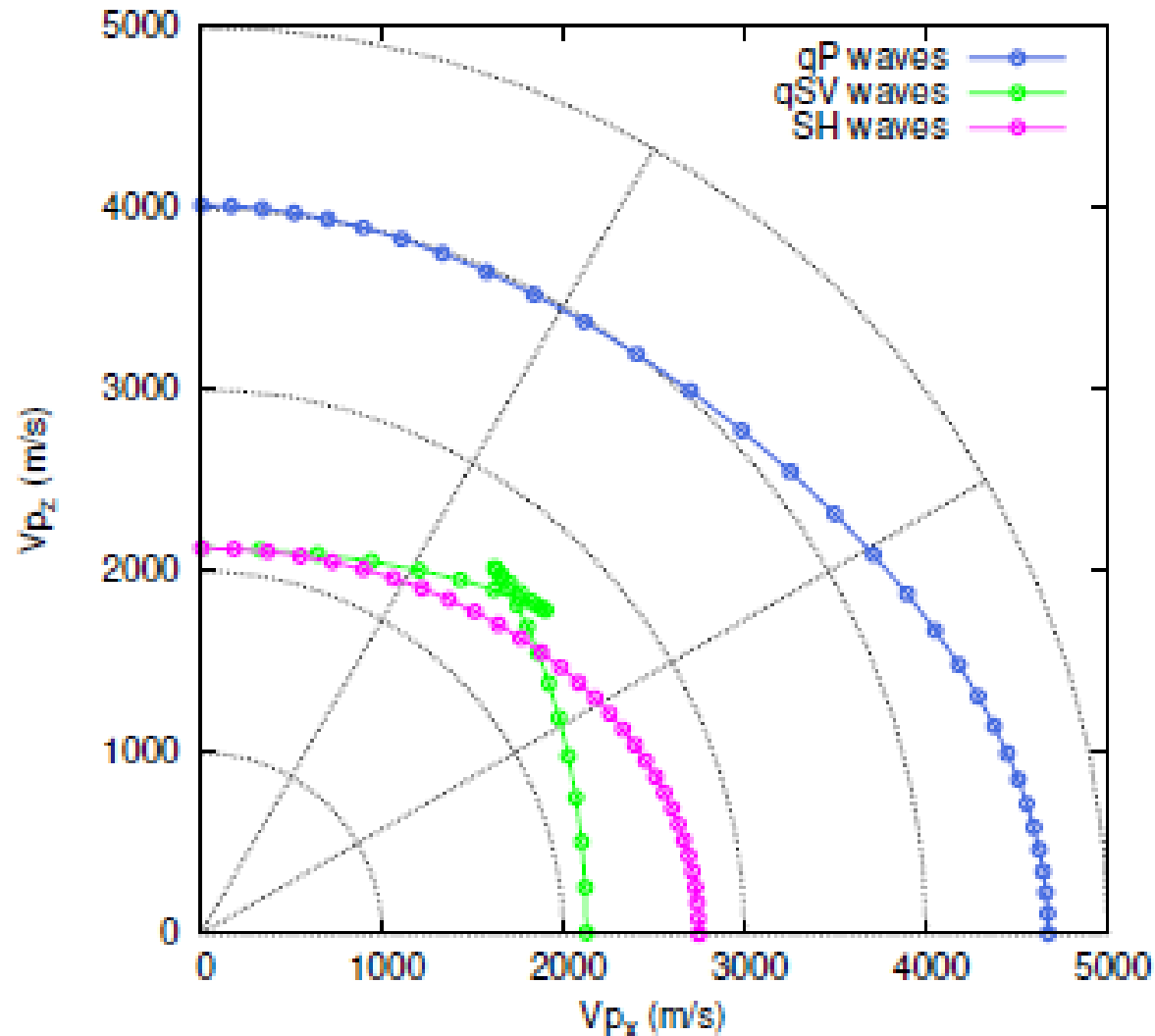


Fig. 3: Polar representation of energy velocities of qP, qSV and SH waves. A notable triplication in the qSV-wave energy velocity pattern can be seen. Frequency is 1 MHz for P-waves and 500 kHz for S-waves.

Well in the VMF from where the core sample was extracted.
Sonic logs.

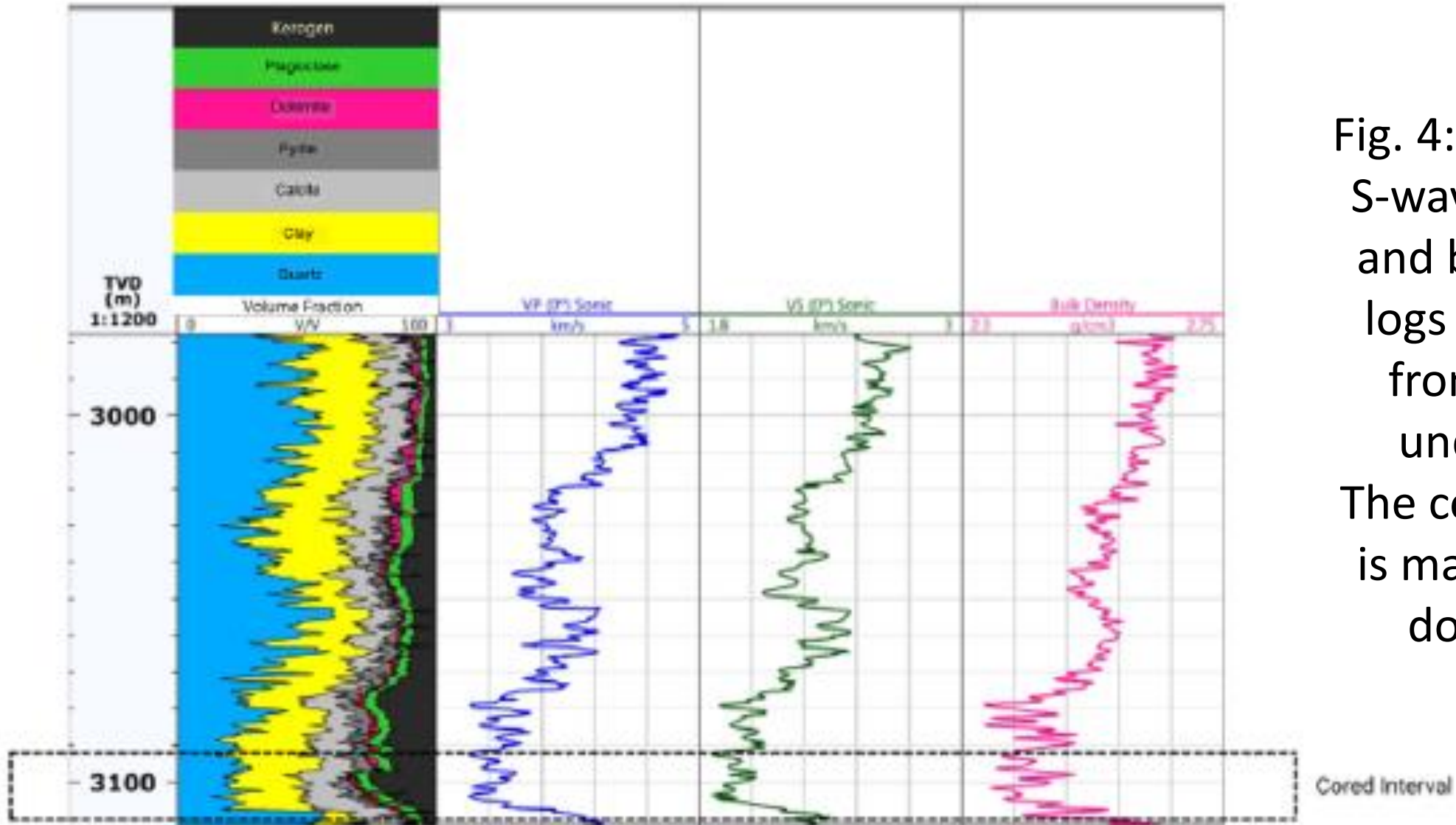


Fig. 4: Sonic P- and S-wave velocities and bulk density logs of the VMF from the well under study. The cored interval is marked with a dotted line.

- Next Figures display phase velocities and attenuation factor $1000/Q$, with Q denoting the quality factor. We consider waves traveling normally to the layering plane ('33' waves).
- For brevity, waves traveling parallel to the layering plane are not shown.
- While phase velocities allows to analyze velocity dispersion for the four saturation scenarios, the attenuation figure allows to study WIFF.

Phase velocity of '33' waves.

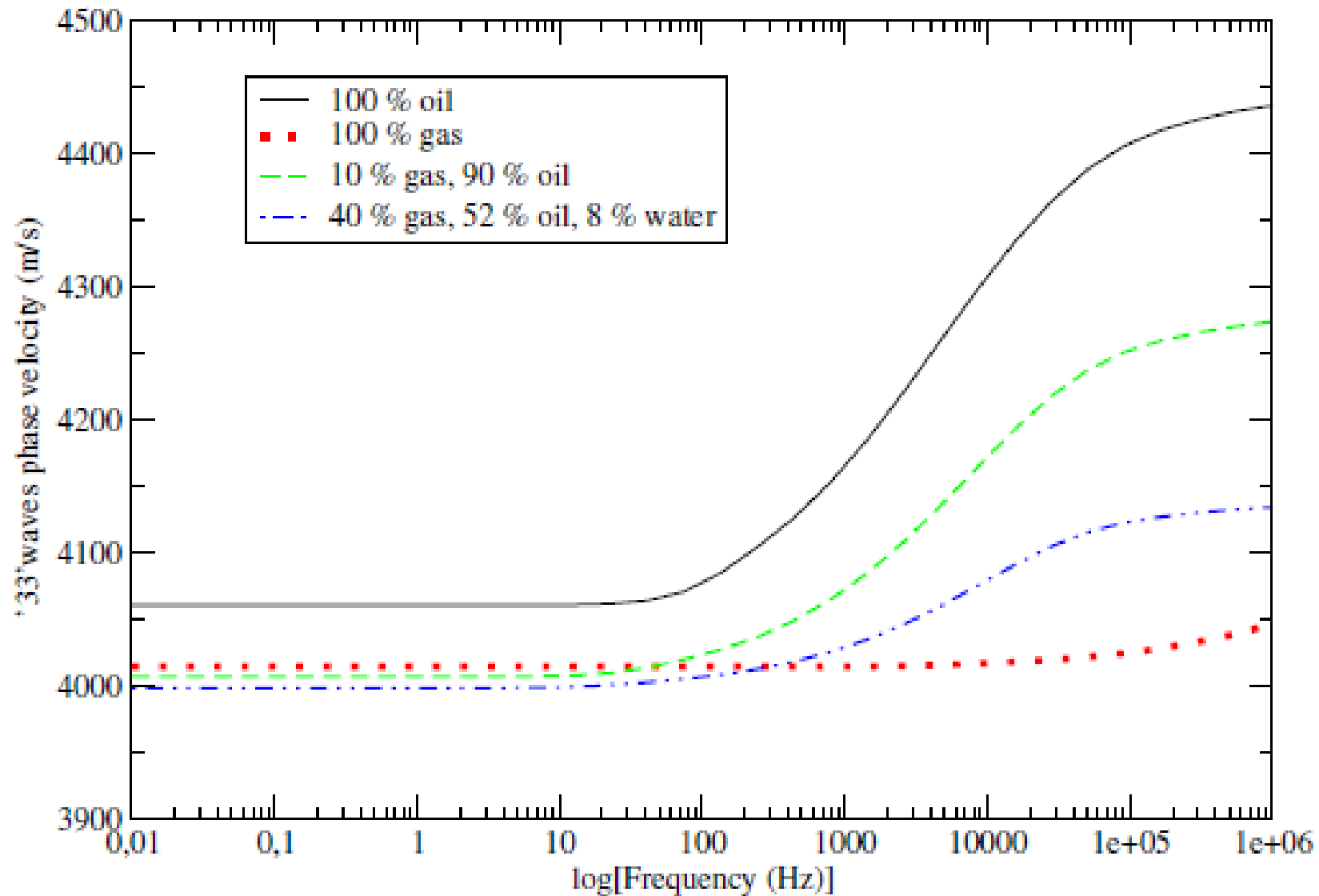


Fig. 5: '33' waves phase velocity as function of frequency.

Attenuation factor of '33' waves'.

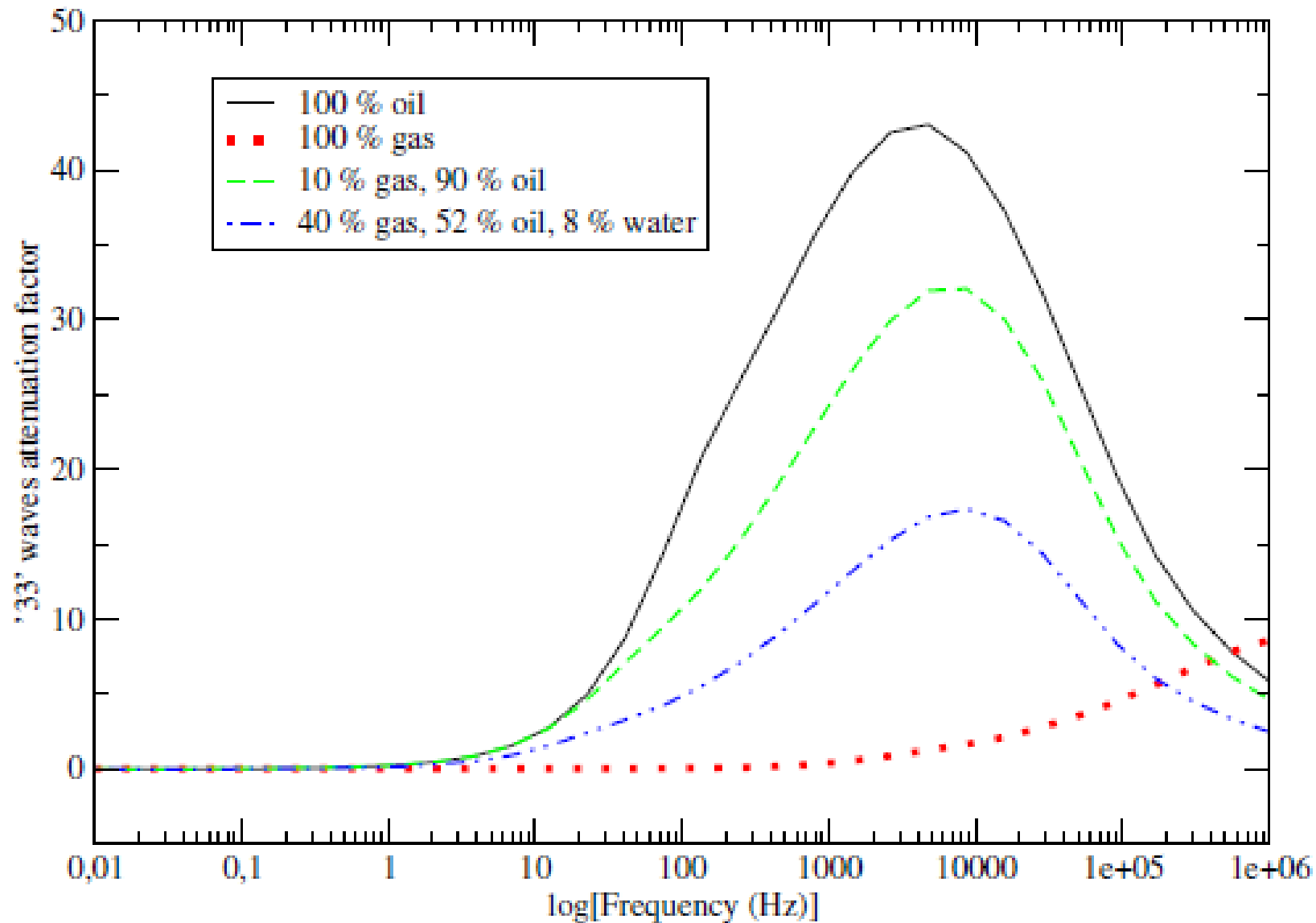


Fig.6: '33' waves phase attenuation factor as function of frequency.

The von Karman self-similar correlation function was used to generate patchy gas-water saturation patterns.

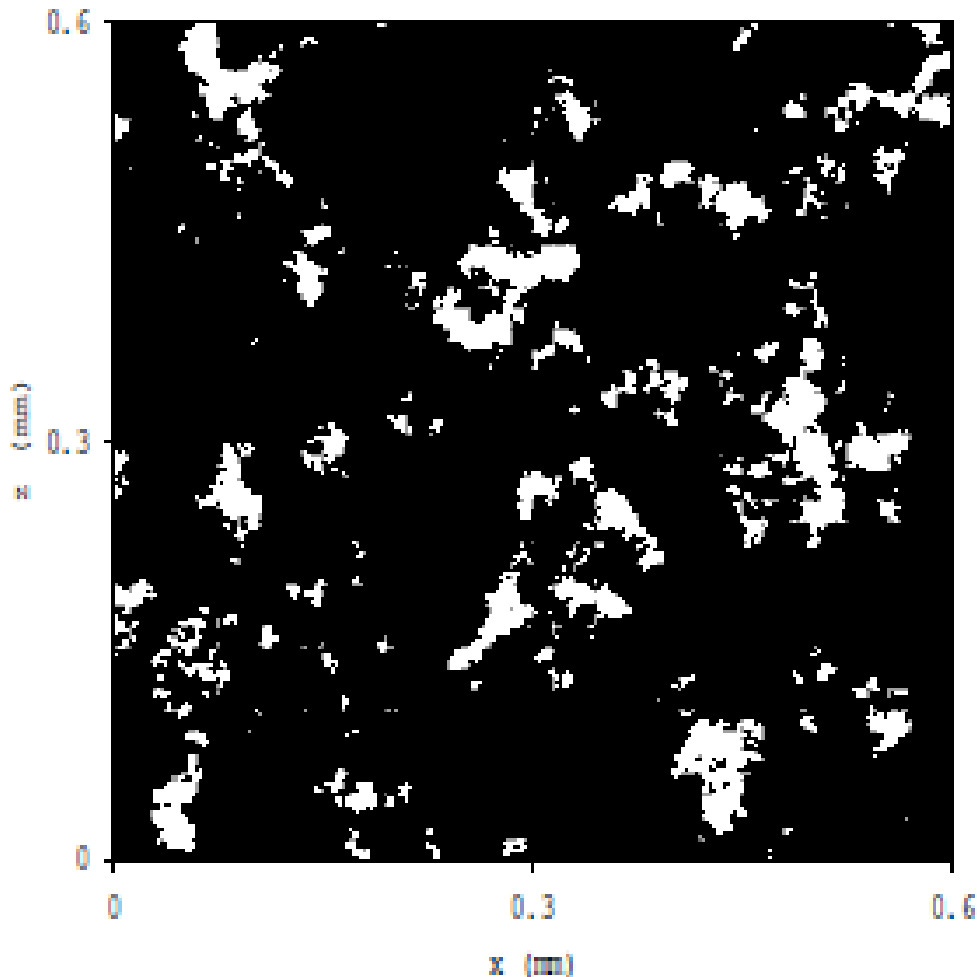


Fig. 7: White zones correspond to full gas saturation and black regions to full oil saturation. Overall gas saturation is 10 percent

Phase velocity of '33' waves for uniform and patchy saturation.

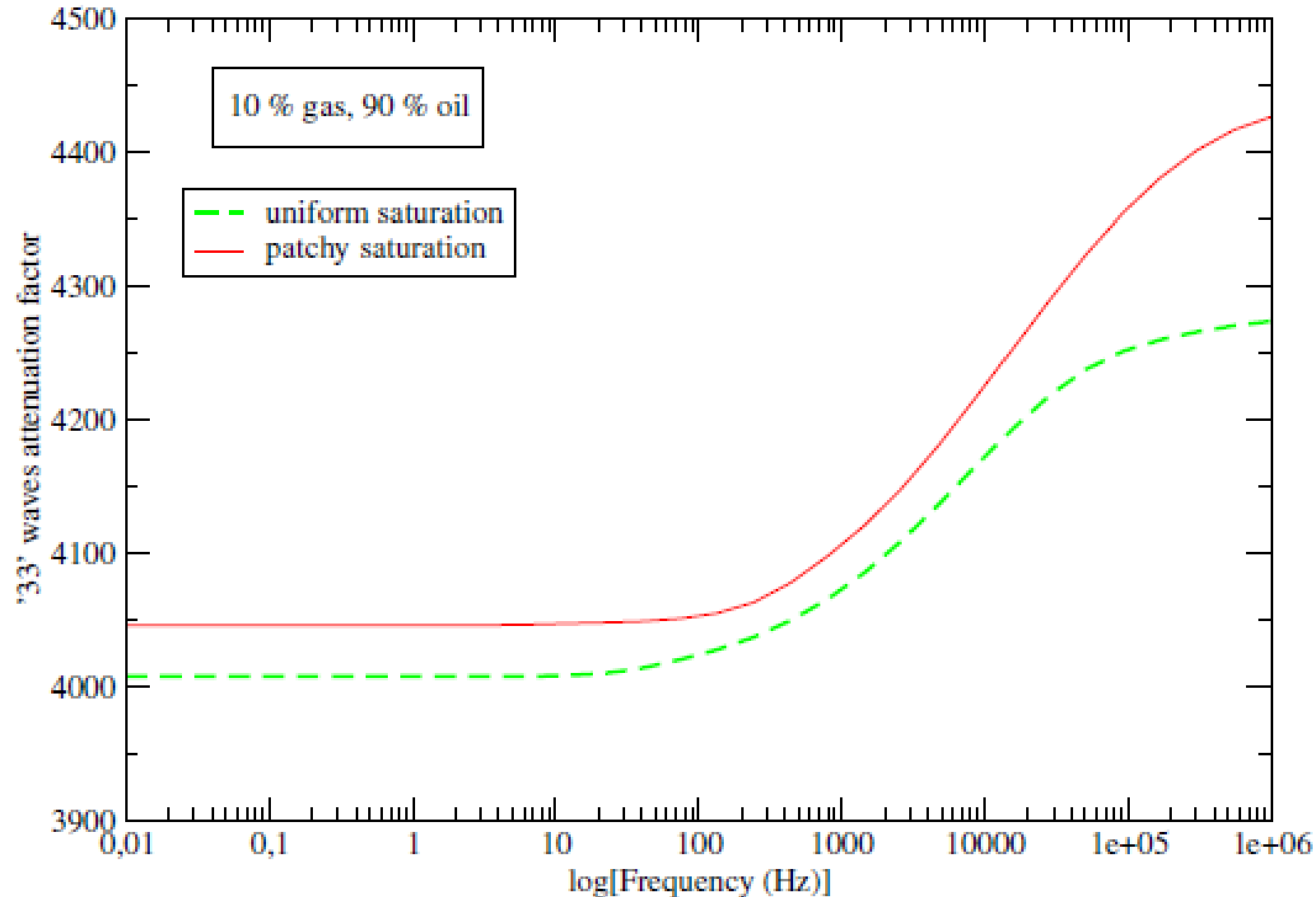


Fig. 8: '33' waves phase velocity for uniform and patchy saturation as function of frequency.

Attenuation factor of '33' waves for uniform and patchy saturation

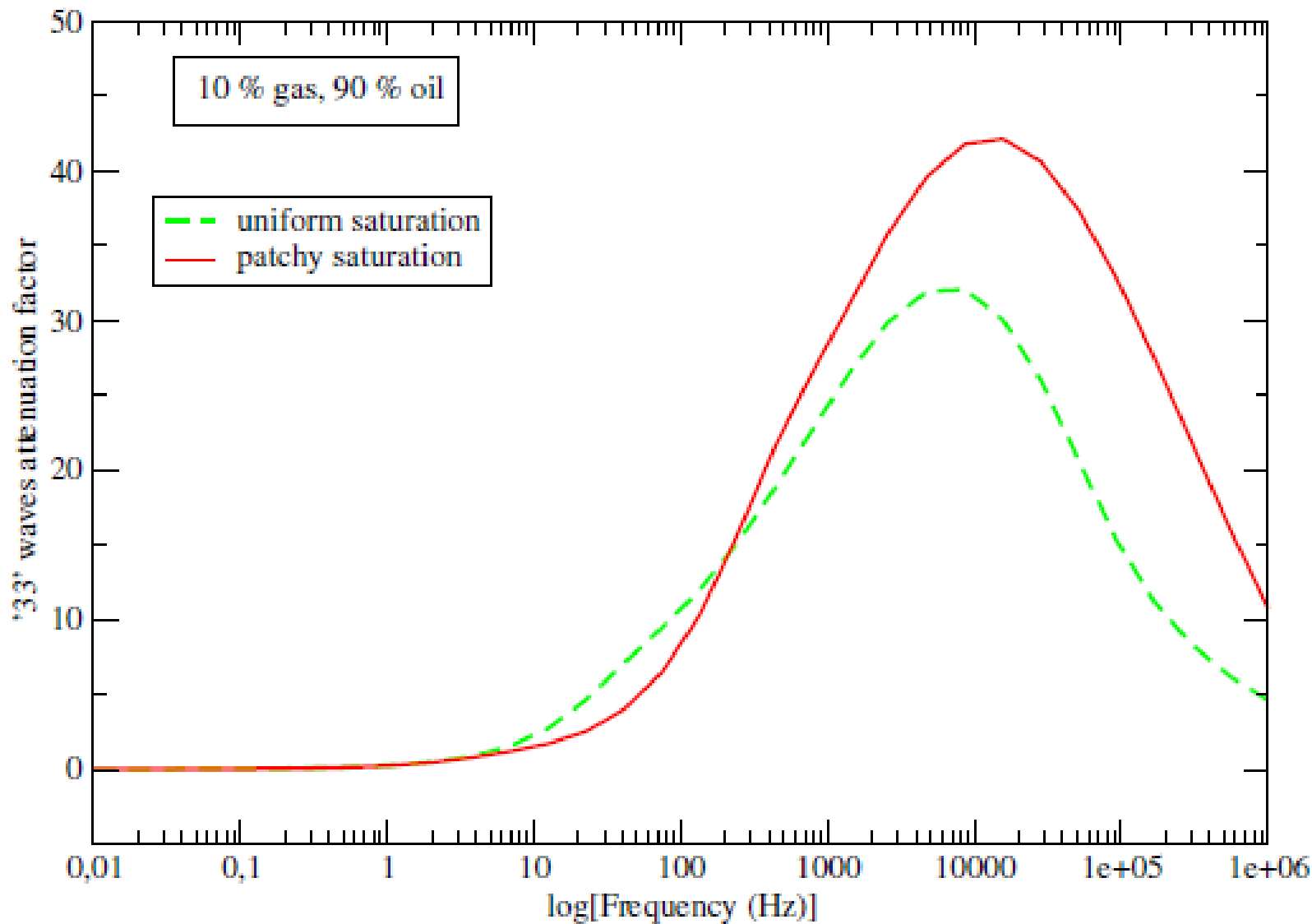


Fig. 9: '33' waves phase attenuation factor for uniform and patchy saturation as function of frequency.

- This study presented a physically grounded, non-phenomenological methodology for estimating the effective anisotropic behavior of the organic-rich mudrock reservoirs.
- The simulations were performed on a finely layered synthetic medium representative of a core sample from the Vaca Muerta Formation.
- The computed phase velocities showed very good agreement with laboratory-measured ones, capturing the strong VTI anisotropy of the formation.
- The inclusion of both patchy and uniformly mixed fluid saturation scenarios emphasized the critical influence of mesoscale fluid heterogeneities on seismic wave dispersion and attenuation.

Estimation of the stiffness tensor in organic-rich mudrock Vaca Muerta by integrating core data with Rock Physics models

THANKS FOR YOUR ATTENTION !!!!!